

Performance of the Xenon Feed System on Deep Space One

Gani B. Ganapathi*

Jet Propulsion Laboratory, California Institute of Technology, Pasadena, California 91109
and

Carl S. Engelbrecht†

PRIMEX Aerospace Corporation, Redmond, Washington 98073

Propulsion for the Deep Space One (DS1) spacecraft is provided by a xenon ion engine. Xenon is stored in a supercritical state and is delivered as a low-pressure gas to the thruster and two cathodes (called the main cathode and neutralizer) by a xenon feed system (XFS). This mission requires tight constraints on thruster performance, which in turn requires separate and very accurate throttling of the thruster and cathode flows; the DS1 spacecraft is the first of its type to utilize a xenon ion engine that can be throttled. Flow is regulated separately to the thruster and cathodes to an accuracy of $\pm 3\%$ using three calibrated flow control devices that are each fed by a dedicated plenum tank. Bang-bang regulators are used to control the set pressures in the plena. The resulting XFS control algorithms are quite complex. The XFS is controlled by a digital control interface unit and the control algorithm for achieving steady-state xenon flow is presented. The worst-case error in flow is shown to be less than $\pm 3\%$, accounting for random and systematic errors. At the time of writing, the individual components are in excellent health and the performance of the XFS is as expected.

Introduction

DEEP Space One (DS1), launched on 24 October 1998 by a Delta II launch vehicle, is the first spacecraft with a throttleable ion propulsion system (IPS) used for primary propulsion. Its primary mission is to validate 12 new technologies of which the IPS is the key one. As part of the primary mission, it flew by an asteroid, 1992 KD, in July 1999. An extended mission is planned for an additional flyby to comet Borrelly in September 2001. (A plan for another flyby to comet Wilson–Harrington in January 2001 has been dropped.) The propulsion system, developed under the Solar Electric Propulsion Technology Application Readiness (NSTAR) program,^{1–4} includes a 30-cm gridded ion engine that is capable of providing a maximum thrust of 92 mN at an I_{sp} of approximately 3100 s. The working fluid for this engine is xenon, stored in a supercritical state to optimize tank mass and volume and delivered at low pressures to the engine by the xenon feed system (XFS). The purpose of this paper is to describe the XFS and detail the performance of the XFS following launch and compare it with what was predicted.

XFS Description and Requirements

The XFS schematic is shown in Fig. 1. Tank T1 was initially loaded with 81.5 kg of xenon; the tank has a volume of 49.62 liters. The initial load pressure at 21°C was 7.577×10^6 Pa (1099 psia). Bang-bang regulators R1 and R2 (each made up of an assembly of two series solenoid valves) are used to regulate pressure in the plenum tanks A1 and A2. The 3.7-liter plenum tanks are required to smooth out the pressure spikes associated with the bang-bang regulators. Latch valves LV3 and LV4 provide a third seal between the high-pressure propellant tank and the low-pressure plena, to assure the prevention of overpressurization of the plena during ground handling. LV1 and LV2 provide on-off control of flow to the engine, and LV5 provides a means of operating the XFS in case of failure in one of the flow branches. (No discussion of off-nominal XFS operation is included here; see Ref. 5 for details.) The flow control devices (FCDs) J1, J2, and J3 are used to regulate the flow

to the engine, and flex lines FL1, FL2, and FL3 are required to allow engine gimbaling. The FCDs are porous sintered metal plugs, and the flow through such a porous plug is a function of pressure and temperature. More details on the flow characteristics for such a device are presented in a later section.

A multidimensional trade study was performed to determine optimized plenum characteristics. Bang-bang regulator manufacturing tolerances and cycle life, range safety considerations, pressure and temperature sensor accuracy, and other variables were considered. The resulting system has a 0.5×10^{-4} liter intersolenoid volume and 3.7-liter plenum tanks with an operating pressure range from 2.76×10^5 to 6.83×10^5 Pa (from 40 to 99 psia) for the main plenum and from 2.76×10^5 to 3.45×10^5 Pa (from 40 to 50 psia) for the cathode/neutralizer plenum.

Each plenum tank is instrumented with a set of three temperature-corrected (hardware and software) pressure transducers [maximum range = 1.03×10^6 Pa (150 psia); accuracy = 0.1% full scale]. The transducers are polled, and the average is used for the control algorithm (discussed later). In the event one transducer from a set drifts significantly from the average, its telemetry is discarded and the average of the other two is used.

The FCDs were procured based on attainable flow accuracy and procurement turn-around time considerations. Turn-around time is very important because the procurement process involves fine tuning the flow rates based on tests, which is an iterative process. The FCDs were flight qualified at the Jet Propulsion Laboratory (JPL), California Institute of Technology. A comprehensive test plan was developed for procuring and calibrating the FCDs for the required flow accuracies. For the sake of brevity, only the error analysis is presented in a later section. Bushway et al.⁶ document more details on the XFS components and the xenon component assembly plate on which the XFS components are assembled.

The key XFS requirements that relate to this paper are shown in Table 1; a full set of requirements is documented in the NSTAR document ND-330 (Ref. 5).

The XFS is capable of providing any desired flow; however, the digital control interface unit (DCIU) is programmed to provide 16 discrete throttle levels. The engine is designed to optimize thrust level based on available solar power. Thus, when the spacecraft is close to the sun, it can throttle at a higher level than when it is farther away. DS1 currently can use only 12 of the available 16 levels due to available power constraints. Figure 2 depicts the mission throttle levels and distance from sun as a function of time after launch. In the next section, the control features of the DCIU are presented.

Received 30 July 1999; revision received 25 February 2000; accepted for publication 25 February 2000. Copyright © 2000 by the American Institute of Aeronautics and Astronautics, Inc. No copyright is asserted in the United States under Title 17, U.S. Code. The U.S. Government has a royalty-free license to exercise all rights under the copyright claimed herein for Governmental purposes. All other rights are reserved by the copyright owner.

*Senior Engineering Staff, M/S 125-109, 4800 Oak Grove Drive; gani.b.ganapathi@jpl.nasa.gov. Member AIAA.

†Project Engineer, P.O. Box 97009, 11441 Willows Road, NE; carlse@red.prmx.com. Member AIAA.

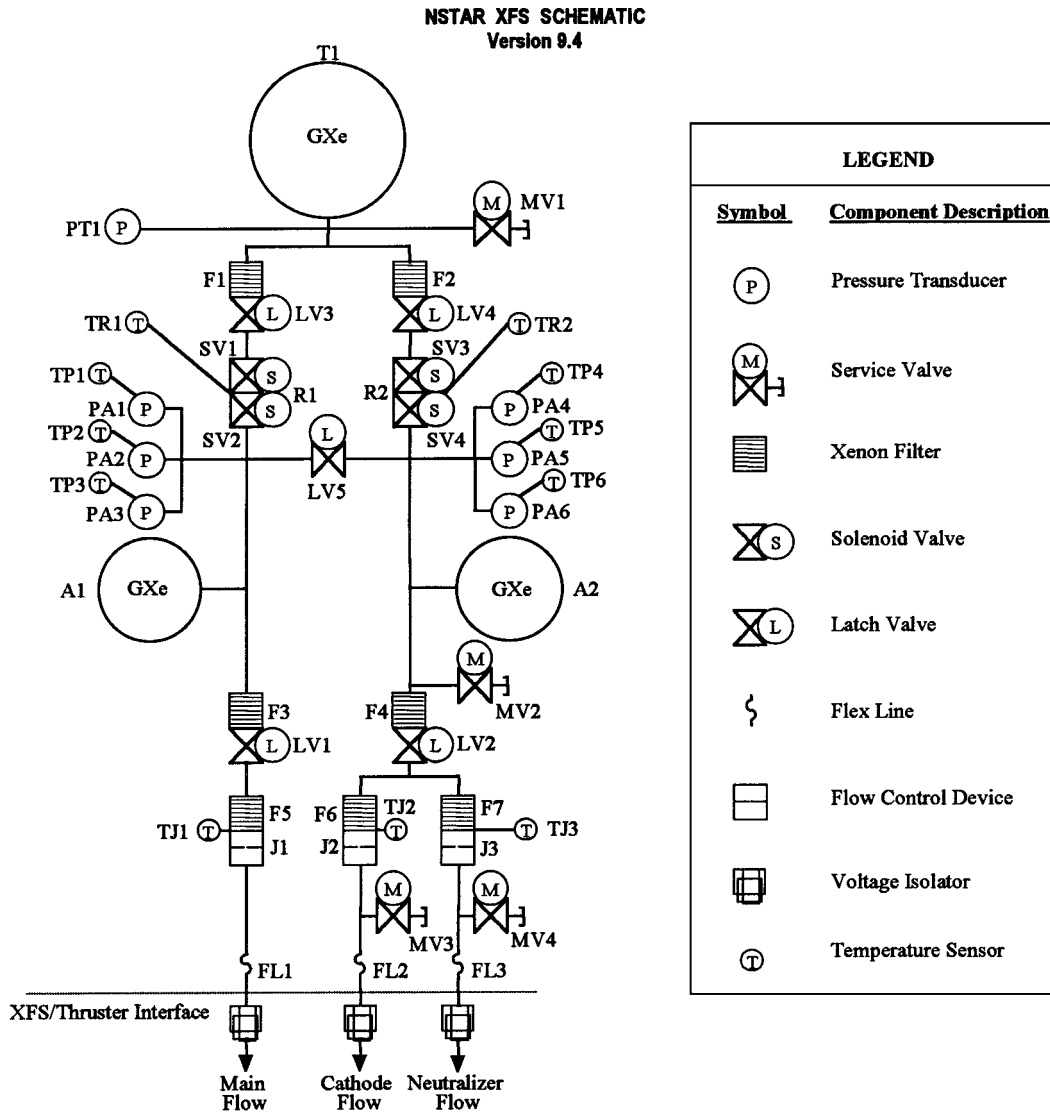


Fig. 1 NSTAR/XFS schematic.

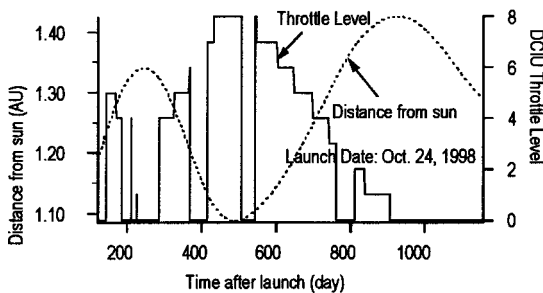


Fig. 2 Throttle level and distance from sun as function of time after launch.

Table 1 Selected requirements for XFS

Parameter	Requirement
Total Xe load, kg	81.5
Flow accuracy	To within $\pm 3\%$ of actual flow
Flow range (16 throttle levels), mg/s	Main inlet: 0.6–2.4 Cathode: 0.25–0.37 Neutralizer: 0.24–0.36
Temperature, $^{\circ}\text{C}$	Range: 20–50 Maximum rate of change: $1^{\circ}\text{C}/10\text{ min}$

Control of the XFS

NSTAR thruster and XFS operations are controlled by the digital control interface unit (DCIU). It is a $\sim 2\text{ kg}$, $30 \times 15 \times 15\text{ cm}$ box utilizing less than 12 W. It is partitioned into 3 VersaModule Eurocard boards: a processor board, a data acquisition board, and a valve driver board. The DCIU controls the XFS using the control algorithm shown in Fig. 3. Note that this control algorithm allows control during steady state and throttling and also has logic to handle fault situations such as leakage or failure of the XFS latch and/or solenoid valves. The fault protection and its responses are beyond the scope of this paper. The DCIU polls all of the XFS temperature and pressure transducers every second, and all telemetry values are updated for control and communication purposes.

The DCIU control algorithm compares the required and measured pressures (both corrected for temperature) and activates the solenoids to pressurize the plena if the measured pressure values are less than the required values. During steady-state operations, the plena are in a continuous state of blowdown, and periodic replenishment via regulator activation is essential to maintain the flow rates. During throttle up, the latch valves LV1 and LV2 can be either closed or open depending on whether the throttling is done prior to starting the engine or while the engine is thrusting. Both throttle modes are allowed by the DCIU. During throttle down, because the required pressure is less than the measured pressure, no action is taken by the DCIU until the pressures match. At this point, the DCIU continues with the normal steady-state control scheme.

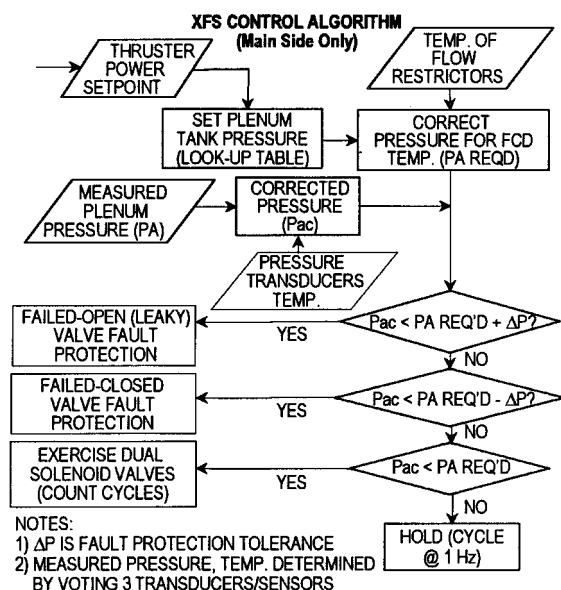


Fig. 3 XFS control algorithm flowchart.

If we refer to Fig. 3, the steady-state DCIU control sequence would be as follows:

1) Ground command determines the throttle level for the spacecraft.

2) Based on the throttle level, a throttle look-up table in the DCIU is used to set the required nominal plenum tank pressures.

3) The nominal required pressures are then adjusted for FCD temperatures. An increase in FCD temperature has to be compensated for by an increase in required pressure and vice versa to maintain a constant flow rate. These adjustments are based on four-point linear interpolations of pressure correction values in the look-up tables; there are two such 16×16 look-up tables in the DCIU, one for each flow branch. A voting scheme is used to determine the average FCD temperature for the correction, where the outlying temperature value is discarded and the average of the best two are chosen. The adjusted required pressure values are called P_A required.

4) A voting scheme similar to that in step 3 is used to determine the temperatures of the pressure transducers. Each of the pressure transducer values is then corrected for temperature using a linear interpolation scheme as in step 3. The corrected pressures on each branch are then averaged using a voting scheme. The averaged measured pressure values are called P_{Ac} .

5) Two fault conditions are then checked for a) overpressurization, when P_{Ac} is greater than P_A required by a predefined limit, and b) underpressurization when P_{Ac} is less than P_A required by a predefined limit. The fault condition limits are not the same.

6) If no fault conditions are met and if the measured pressures are less than the required ones, then the solenoids are activated to pressurize the plenum tanks.

Pressurization of a plenum tank is achieved by sequential activation of the pair of solenoid valves in the regulator as mentioned before. High-pressure xenon trapped within the intersolenoid volume following an open/close cycle of the upstream solenoid is injected into the plenum tank when the downstream solenoid is cycled opened/closed. The required open times of the upstream and downstream solenoids are a function of many parameters such as supply xenon pressure and temperature, solenoid temperature, and plenum tank pressure and temperature. It is important to optimize the solenoid cycle times because mission pressurization times can be impacted, particularly later in the mission when many regulator cycles are required to pressurize the plenum tanks due to lower xenon pressure in the supply tank. Optimal open times are shown in Fig. 4.

In Fig. 4, the plenum pressure is assumed to be 2.86×10^5 Pa (41.5 psia), which is representative of the lowest pressures to be seen in the plenum tanks. A worst-case γ (c_p/c_v) = 1.7 was assumed for all of the calculations. Also, uniform temperatures for

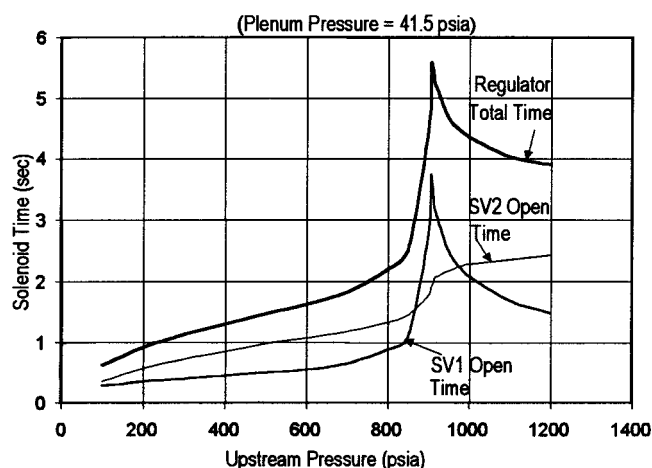


Fig. 4 Optimal solenoid open times as function of supply pressure.

all components were assumed. Clearly, the optimal required open times passes through a peak around the critical pressure of xenon. Testing with an engineering model of the XFS verified these trends and experimental values were close to model predictions. To ascertain that the XFS would satisfy the requirements imposed on it, an error analysis was conducted. The results are presented in the next section.

Feed System Flow Uncertainty

The flow uncertainty of the XFS is made up of systematic and random error components. The systematic error would constitute items such as pressure transducer drift and sawtooth error due to the pressure profile within the plenum caused by the bang-bang regulator operational characteristics. Random errors are due to uncertainties in the transducers, calibration, modeling, etc. The systematic errors are typically additive and the random errors are root mean squared together. Figure 5 depicts the contributions due to random and systematic errors.

The FCD characterization error is discussed first because this is the most involved. JPL's FCD test stand utilizes mass flowmeters, which are calibrated prior to each FCD characterization. The calibration system, which is a primary standard traceable to National Institute of Standards and Technology (NIST), measures flow in the $1\text{--}50,000$ standard cm^3/min range with an accuracy of 0.2% of flow over the entire range. The calibration procedure involves automatically recording voltages indicated by the mass flowmeter, as well as the temperatures and test pressures. The flowmeter is calibrated over a range of flow rates and pressures representative of flight conditions. For all of the tests, mass flowmeters were utilized; however, different units were used to measure main and cathode flows. The uncertainties associated with the different elements in the calibration process are calibration system, $\pm 0.2\%$ of flow; voltage uncertainty, $\pm 0.1\%$; calibration curve fit error, $\pm 0.26\%$; and temperature correction, $\pm 0.15\%$.

The resulting flow calibration uncertainty σ_{calibr} is equal to $\pm 0.37\%$ (the root mean square of the aforementioned components).

With a calibrated mass flowmeter, the FCDs were characterized with temperatures ranging from 20 to 50°C and upstream pressures ranging from 2.41×10^5 to 6.83×10^5 Pa (from 35 to 99 psia) for main and from 2.41×10^5 to 5.17×10^5 Pa (from 35 to 75 psia) for cathode FCDs. The downstream pressure was maintained below a few torr in all cases.

The flow characteristic of a porous plug such as the one used can be modeled as

$$\frac{p_1^2 - p_2^2}{L} = \frac{2\alpha RT \mu G}{M g_c} + \frac{2\beta RT G^2}{M g_c} \quad (1)$$

In Eq. (1), p_1 and p_2 are upstream and downstream pressures, respectively, G is the superficial mass velocity, g_c is a dimensionless constant, M is the molecular weight, R is the gas constant, T

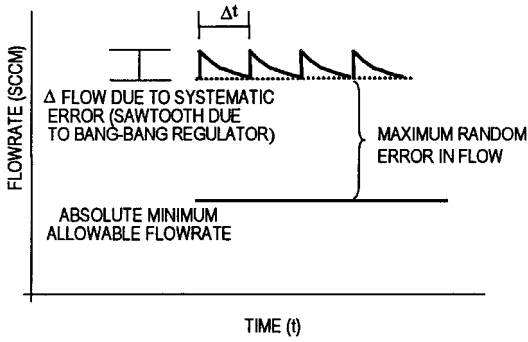


Fig. 5 Systematic and random errors in flow.

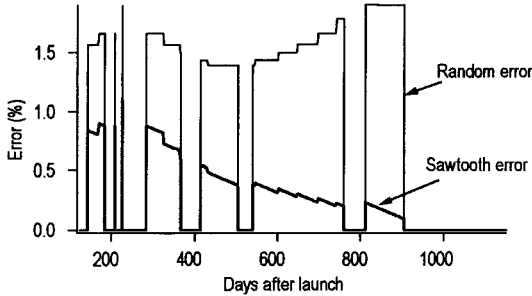


Fig. 6 Random and systematic error components of flow over mission (main side).

is absolute temperature, α and β are constants representative of the porous plug, and μ is the viscosity of the gas. However, this model was not adequate because the error in fit was almost $\pm 2\%$. An alternate nonphenomenological model was, therefore, developed with a curve fit error less than $\pm 0.8\%$ over the entire range of pressures and temperatures. The model was of the form

$$\begin{aligned} \text{Flow}(\text{pressure, temperature}) = & a_0 + a_1 \times \text{pressure} + a_2 \times \text{pressure}^2 \\ & + a_3 \times \text{pressure}^3 + a_4 \times \text{temperature} + a_5 \times \text{pressure} \\ & \times \text{temperature} + a_6 \times \text{temperature}^2 + a_7 \times \text{pressure}^2 \\ & \times \text{temperature}^2 + a_8 \times \text{temperature}^3 \end{aligned} \quad (2)$$

Equation (2) also has the advantage of being explicit in flow with the caveat that the downstream pressure is below 5.33×10^3 Pa (40 torr).

When the uncertainties in test stand pressure and temperature sensors are included, the model uncertainty is given by

$$\sigma_{\text{model}} = \sqrt{\sigma_{\text{model, fit}}^2 + \sigma_{\text{temp}}^2 + (2\sigma)_{\text{press}}^2 + \sigma_{\text{calibr}}^2} \quad (3)$$

The terms in Eq. (3) are nondimensional fractional errors. Thus, $\sigma_{\text{temp}} = \Delta T / T$, etc. Note that in Eq. (3) any uncertainty in the pressure will result in an approximately twofold increase in flow uncertainty due to the approximately parabolic nature of the flow-pressure curve in the regime of interest.

The uncertainties in test stand pressure and temperature are ± 689 Pa (± 0.1 psi) and $\pm 0.5^\circ\text{C}$, respectively. Thus, for a worst-case pressure of 2.76×10^5 Pa (40 psia) and 20°C (293 K), the model uncertainty is $\sim \pm 1.2\%$.

In flight, the flow uncertainty is a function of the preceding model uncertainty of $\pm 1.2\%$ and plenum pressure and FCD temperature sensor uncertainties that are $\pm 2.07 \times 10^3$ Pa (± 0.3 psi) and $\pm 1^\circ\text{C}$, respectively; the corresponding worst-case rms flow uncertainty due to random errors is $\sim \pm 1.9\%$.

The sawtooth error component is additive to the random error and, when averaged over many regulator cycles, the maximum sawtooth error can be as high as $\pm 1\%$ of flow. Thus, the total worst-case uncertainty in flow is $\pm 2.9\%$. The actual error will be less and is shown in Fig. 6 as function of mission profile.

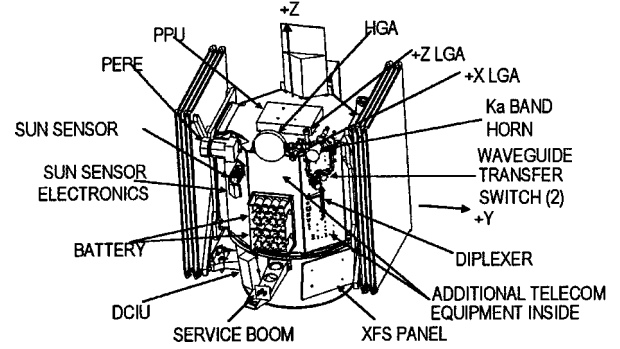


Fig. 7 Location of XFS and DCIU on spacecraft.

From Fig. 6, it can be seen that as the mission progresses, the systematic error due to sawtooth decreases, as one would expect, due to lower pressure slugs being used to pressurize the plena. The random error can be seen to be a function of the throttle level, with lower pressures contributing to larger uncertainties in flow (see Fig. 2 for throttle levels). However, the maximum error is less than 1.9% as mentioned earlier. Regions where the errors are zero correspond to times where there is no thrusting and, hence, no flow.

In this error analysis it is assumed that the pressure transducer drift is zero, which may be valid only for the early stages of the mission; however, the sawtooth error decreases as xenon is consumed and will partly compensate. The true error will be unknown because there is no absolute measurement against which to determine pressure transducer drift in flight.

XFS Postlaunch History

The DS1 spacecraft was launched on 24 October 1998. Two days after launch the DCIU was turned on for the first time. Postlaunch telemetry indicated that all XFS valves were in the closed state as expected and that the XFS pressures and temperatures were within expected ranges. Four days after DCIU turn-on, on 30 October, the first XFS activity, FCD calibration, was started. To verify that the FCD calibrations did not shift as a result of launch, a plenum blowdown test was performed. In this mode, only latch valves LV1 and LV2 were opened to initiate xenon flow through the FCDs. The plenum pressures and temperatures were monitored over an 8-h period, and the pressure profiles were compared with expected values. Prior to the start of the test, the thruster was turned 30 deg off-sun. (See Fig. 7 for axes, thruster, XFS plate, and DCIU locations on the spacecraft.) The turn to sun was carried out to heat up the lines in the spacecraft to help outgas any adsorbed water in the lines following launch. (Cathode life is significantly affected by exposure to contaminants such as water and oxygen.)

On 9 November 1998, the thruster was turned on for the first time in diode mode. In this mode, xenon flow is initiated and ionization of the gas occurs; however, the ionized gas is not accelerated through the grids and, hence, no effective thrust results. The engine was run in this mode to outgas any remaining water in the thruster area. On 10 November the engine was turned on to start acceptance test 1. This test was designed to test all of the IPS subsystem performance parameters at six different throttle levels. However, after running nominally for 4.5 min, the engine shut itself off and could not be turned back on despite thermal cycling and multiple restart commands. The DCIU was then turned off on 11 November and was turned back on 24 November to conduct additional thruster diagnostics. When the engine was commanded to turn on, it started up and since then has continued to perform flawlessly. On 30 November the rescheduled acceptance test 1 was conducted, and a significant amount of data were gathered to determine the performance of the IPS. The results are presented in the following sections.

XFS Component Status

Latch Valves

LV1–LV4 have been cycled less than 100 times at the time of preparing this document (May 1999). They have been qualified for over 12,000 cycles. LV5 has not been cycled in flight, this valve will

only be used in the case of a fault. The prelaunch measured internal leakage rate for all latch valves were at least two orders of magnitude less than the required 1×10^{-3} standard cm^3/s . For postlaunch, the pressures in the plenum tanks were followed for a period of 2 weeks where there was no thruster activity (10–24 November 1998). Subsequent telemetry also indicated no leakage. During this time there was no discernible change in the pressures, which led to the conclusion that LV1, LV2, and LV5 were not leaking. Conclusions on integrity of LV3 and LV4 were possible only by inference but could not be proven due to the presence of solenoid valves SV1–SV4.

Pressure Transducers

The supply pressure transducer is 2.07×10^7 Pa (3000 psia) full scale with a rated accuracy of $\pm 1.0\%$ FS (2.07×10^5 Pa, 30 psi) without a calibration look-up table. However, with the loaded calibration data in the DCIU, the accuracy is ± 6895 Pa (± 1 psi). Any drift can be detected by comparing calculated xenon consumption by integration of flow with expected pressure at a given temperature.

There are six 1.03×10^6 Pa (150 psia) low-pressure transducers for the plena with three on each plenum with a rated accuracy of $\pm 0.1\%$ FS with the calibration look-up table. Component acceptance tests indicated that PA5 indicated a lower pressure than the other two cathode transducers by approximately 1.38×10^3 Pa (0.2 psi). XFS functional testing indicated that in addition to PA5, PA1 on the main plenum also indicated a slightly low pressure. As a result, the XFS is flowing a bit rich, with an expected impact of 0.25 kg extra propellant use in the mission. The current thought is to change the calibration on these pressure transducers at a later time in flight to rectify the problem.

Regulators

The regulators RG1 and RG2 have been cycled 15,200 and 5500 times, respectively, to date and are functioning nominally. No internal leak is discernible. A conservative 4-s open time was chosen for the DS1 initial setting. This will be reduced as the mission proceeds. The duty cycle of the regulator is a variable that can be modified by changing the delay time between solenoid activation. Currently, the DS1 is operated at a 25% duty cycle (total regulator time = two solenoids \times 4 s open time per solenoid/25% duty cycle = 32 s) to minimize thermal impacts.

Temperature Sensors

There are a total of 13 temperature sensors in the XFS: in the supply tank, 1 ($\pm 1.7^\circ\text{C}$); in the regulators, 2 ($\pm 0.4^\circ\text{C}$); in the plenum tank (only main plenum tank instrumented), 1 ($\pm 1.7^\circ\text{C}$); in the FCDs, 3 ($\pm 0.4^\circ\text{C}$); and in the pressure transducers, 6 ($\pm 5^\circ\text{C}$).

The FCD and regulator temperature sensors are 500- Ω platinum resistance thermometer devices (RTDs) and are the most important ones. The temperature sensors within the pressure transducers are 100- Ω platinum RTDs and are not critical because the pressure transducers are internally temperature compensated with software-based corrections needed only for large changes in temperature ($\Delta \sim 15$ – 20°C).

All of the temperature sensors with the exception of the supply tank temperature sensor (telemetry channel V-4054) are functioning nominally. V-4054 was noted to have started drifting from the expected range 25 – 28°C (due to heater cycling) to 28 – 31°C . Fortunately, IPS operations are not impacted in any way, and this channel is not used for xenon mass calculations either, because better means exist (discussed hereafter).

XFS Performance

Analytical models have been developed for different purposes during the design, assembly, test, and mission operation phases of the XFS.

Because the storage and utilization of supercritical xenon was involved, it is important to understand the thermodynamics of xenon and its impact on flight operations. The behavior of xenon is best understood with the help of Fig. 8.

For a loading of 81.5 kg, the tank pressure will be 8.41×10^6 Pa (1220 psia) at 25°C (between 20 and 30°C). At this pressure and

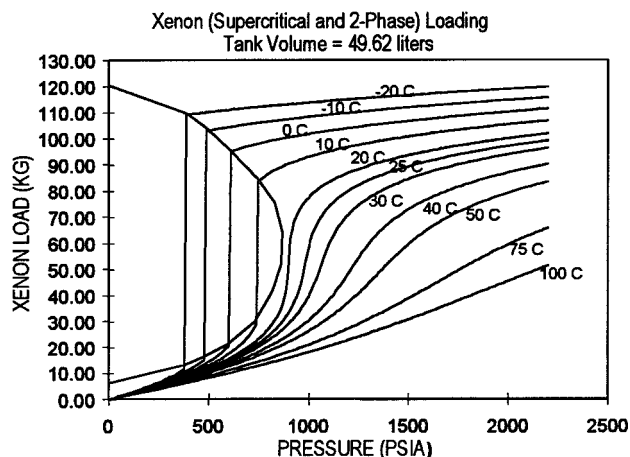


Fig. 8 Phase diagram of xenon.

temperature, xenon is supercritical. However, as the xenon in the tank approaches 60 kg, it can be seen that the density/pressure profile becomes very steep, particularly for isotherms close to 16.7°C , because the xenon is close to its critical state. Very slight changes in temperature cause large shifts in density/pressure. Also, small uncertainties in pressure transducer readings can lead to large mass estimation errors. It is important to avoid the two-phase boundary for many reasons, hence the requirement for the lower flight temperature bound of 20°C stated earlier.

The equation of state for xenon can be represented in many different ways such as the virial equation of state, van der Waals, etc.⁷ However, these equations were found to be inadequate for the accuracies required, and they are implicit when solving for specific volume (or density). This places a severe constraint for many calculations where density is calculated repetitively because it impacts both computational time and accuracy due to propagation of small errors.

The approach used for all XFS analysis was to use the NIST thermophysical properties software that utilizes a 32-term modified Benedict–Webb–Rubin equation of state.⁸ Typical uncertainties in the calculated standard reference data are about 0.1–0.3% in density, 0.5–2% in enthalpy, 2–5% in heat capacities, 2% in viscosity, and 4–6% in thermal conductivity over a broad range of state variables. Figure 8 was generated using the NIST software.

The following performance models were developed for the XFS: 1) FCD calibration, 2) optimal regulator open time, 3) temperature correction algorithm, 4) throttling up and down, and 5) xenon consumption as function of mission.

In this section, comparisons between expected and actual flight data will be presented where applicable. For example, no flight data are available to validate optimal regulator open time; however, verification has been performed at the engineering model feed system level. The xenon consumption model has been validated for the mission so far.

FCD Calibration

Prelaunch calibrations of the FCDs were performed on 5 March 1998. Both plena were pressurized to $\sim 5.17 \times 10^5$ Pa (75 psia), and latch valves LV1 and LV2 were opened to initiate flow. After 8 h the latch valves were closed again. The average temperature of the FCDs during this period was $\sim 21^\circ\text{C}$. The DCIU was turned off for some portions of the test as there were some spacecraft-critical activities that demanded it. Postlaunch FCD calibrations were performed on 30 and 31 October 1998. The initial pressures in both tanks were $\sim 6.83 \times 10^5$ Pa (99 psia) and total period of flow was for 22 h. There were significant variations in temperatures (28 – 36°C) in the FCDs due to the turn to the sun mentioned earlier. Comparisons between pre- and postflight calibrations are presented in Figs. 9 and 10 in the common pressure ranges.

The aforementioned comparisons show some deviation between actual pre- and postlaunch pressure profiles due to different temperatures; however, the model matches the postlaunch data very well.

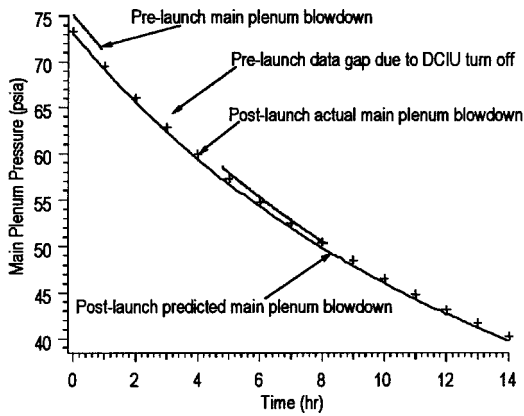


Fig. 9 Comparison of pre- and postlaunch main FCD calibration with expected values.

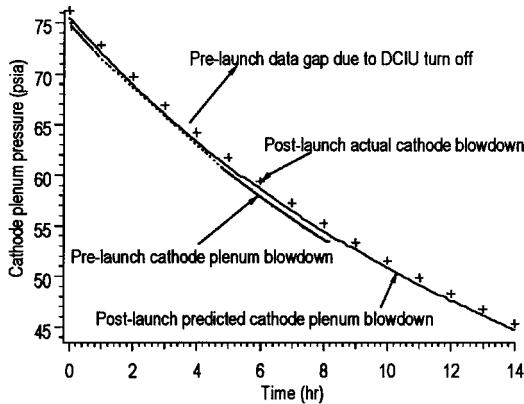


Fig. 10 Comparison of pre- and postlaunch cathode FCD calibration with expected values.

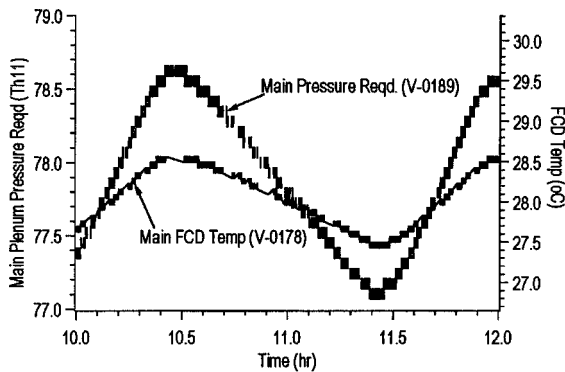


Fig. 11 Telemetry data for temperature correction algorithm (main FCD).

Temperature Correction Algorithm

As mentioned in the section for control of XFS, the DCIU is loaded with two 16×16 temperature correction tables for the main and cathode plena to set the required throttle pressures that account for varying FCD temperatures. If the temperature was steady at 21.1°C (baseline temperature), the required main plenum pressure would be 5.244×10^5 Pa (76.06 psia) for a flowrate of 18.51 standard cm^3/min . However, because the temperature fluctuates between 27.5 and 28.5°C , the required pressure fluctuates between 5.31×10^5 Pa (77.0 psia) and 5.43×10^5 (78.7 psia) as seen in Fig. 11.

Throttling Up

The model for predicting the time required for throttling up is based on knowledge of supply temperature and pressure, regulator temperature, and plenum pressure and temperature. With latch valves LV1 and LV2 closed, the model prediction has been to within a few percent of actual flight data; however, when the throttling is performed with the engine thrusting, the model prediction is not bet-

ter than 15%. For example, the predicted number of cycles needed to throttle up from throttle level 6 to 9 when thrusting was 25, whereas the actual number was 30. Thus, the model prediction is slightly off under thrusting conditions, but this has no impact on flow performance. The reason for the discrepancy has not been established. Figure 12 shows an example of throttling up performed in acceptance test 1.

Throttling Down

When the spacecraft throttles down to a lower throttle level, the plena continue to bleed down until the desired pressure is reached. The regulation algorithm then kicks in to maintain the pressures. An example of throttling down from throttle level 12 to 11 is shown in Fig. 13. The actual time for throttle down matches prediction to within a few percent.

Note the following from Figs. 13 and 14:

- 1) The throttle up time is much faster than throttle down time. Each throttle down event is associated with a finite xenon loss, as the plenum tank pressure decreases to its target value, which is not useful for thrusting.
- 2) The setpoint for triggering the plenum repressurization is set such that at no point is the cathode or main flow less than nominal. This is because cathode life is significantly affected by flow starvation. There is some loss associated with these sawtooth pressure and flow spikes; however, the loss over the mission is not significant (discussed later).

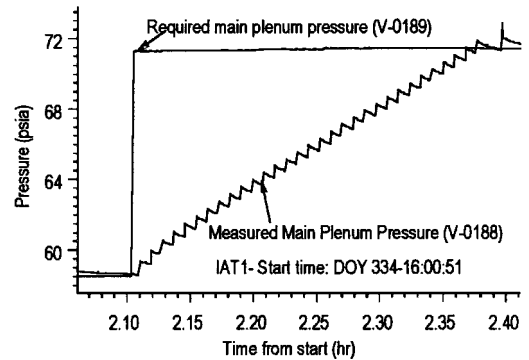


Fig. 12 Telemetry data for throttle up from 6 to 9.

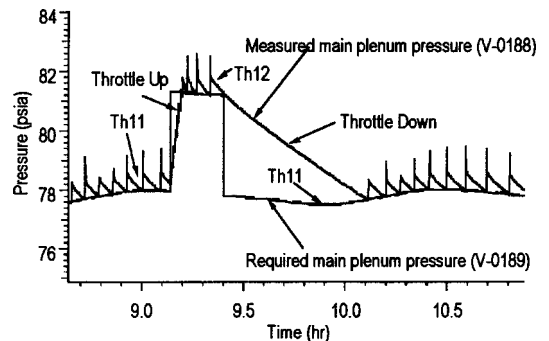


Fig. 13 Throttling down from throttle level 12 to 11.

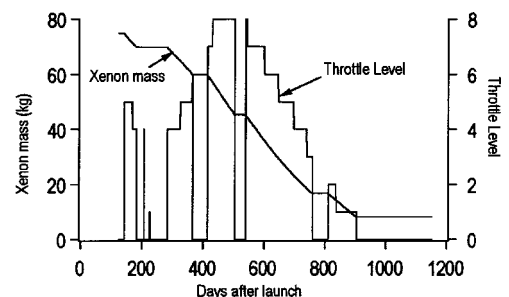


Fig. 14 DS1 throttle level and xenon mass profile.

Polling Algorithm

The polling algorithm for the plenum pressure transducers was designed to account for possible drifts in the transducers. The current algorithm first averages all of the three transducers in each branch. Then, if any of the transducers' value is different from the average by 0.5%, that transducer value is discarded and the average of the other two are used. In the current implementation, 6.34×10^3 Pa (0.92 psi) was used as a cutoff. However, this tolerance will be narrowed in future to 3.45×10^3 (0.5 psi).

The polling algorithm tries to do a good job in the face of many possibilities. However, it needs further attention, particularly on how to handle transducers that have an offset since launch. One way, as mentioned earlier, would be simply to change the calibration of the erring transducer because the offset is constant at all pressures. The polling algorithm is currently causing the xenon flow to be a bit richer than required, which will impact the xenon inventory by approximately 0.25 kg if left uncorrected.

Mission Profile and Xenon Consumption

The optimal trajectory for the flyby of the asteroid is based on available solar power and thrust, and the mission is designed accordingly. The xenon consumption is a function of throttle level and duration of burn. Figure 2 showed the variation of distance from sun and thrust levels. As the distance from the sun increases, the amount of power available to the solar panels decreases, and, hence, lower thrust levels are available.

With the knowledge of mission thrust profile, it is possible to estimate the amount of xenon consumed through the mission. The estimated xenon consumption profile is shown in Fig. 14. Although integration of nominal mission flow rates is the only way to estimate future xenon consumption, there are other techniques to estimate current available xenon in the supply tank. One way would be to count the number of solenoid cycles and another would be to track the supply tank pressure and temperature and estimate mass from an equation of state. However, both approaches face problems related to the supercritical storage of xenon and are used only as backup techniques. Calculation of xenon density is required to calculate the xenon mass using the solenoid count and equation of state estimate approaches.

As the xenon pressure in the supply tank approaches the critical value, very small errors in pressure and/or temperature estimates lead to large errors in mass calculations; for example, an error in pressure of 3.4×10^4 Pa (5 psi) and an error in temperature of 1°C around the critical point could lead to an error of up to 18 kg in mass calculations.

Predicted values of xenon consumption for the mission are based on nominal flow rates; however, actual xenon consumption values are obtained by integration of flows calculated from plenum pressures and FCD temperatures. As an example, Fig. 15 shows a close-up view of the integration for mass consumption over approximately 1.5 h. Note that Fig. 14 was based on the latest mission profile and starts from day 125 (27 February 1999); 6.6 kg of xenon was consumed prior to this period.

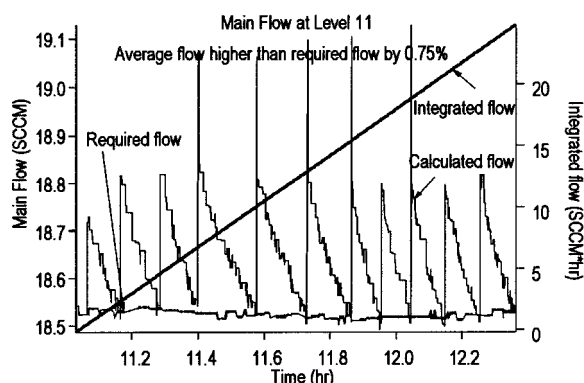


Fig. 15 Close-up of integrated main flow.

For conversion, one can use the relationship 1 standard cm^3/min (sccm) = 0.09838 mg/s to determine the amount of xenon consumed. Thus, in Fig. 15, $24.66 \text{ sccm} \cdot \text{h}$ corresponds to 8.73 g consumed in a 1.5-h period. The sharp sawtooth profile on average increases the nominal flow by 0.75%. The sawtooth error is a function of many factors such as amount of xenon in the supply tank, plenum tank pressure, and temperatures. As the mission proceeds, and as xenon is consumed, this error decreases.

Conclusions

This paper has focused on performance related issues of the XFS used on DS1. The XFS design has been shown to be adequate to provide xenon over the full throttling range of the IPS. In addition, the required flow accuracy of $\pm 3\%$ has been achieved over the entire throttling range. The control algorithms coded into the DCIU have been shown to be robust and capable of throttling up and down to the desired setpoints accounting for temperature changes. All of the components are functioning nominally with the exception of calibration offsets in two of the low-pressure transducers and drift in the high-pressure transducer. Future changes to the XFS envisioned include changing the faulty calibration on the two low-pressure transducers, changing the solenoid open times and regulator delay times to account for decreasing xenon supply pressure, and changing the setpoint for plenum pressurizations such that on average the flow rate is nominal.

In conclusion, we are gratified to note that the XFS is performing well. In addition, the models developed to predict the performance have proven to be very accurate, and this has been a source of satisfaction to the authors.

Acknowledgments

We wish to thank our industrial partners at Moog, Inc., who helped us assemble the Xenon Component Assembly and provided many of the components. Non-Moog components were the pressure transducers, produced by Taber, the FCDs, produced by Mott, the supply tank, produced by Lincoln Composites, the plenum tanks produced by SCI, and the RTDs, produced by Rosemount. We extend thanks to John F. Stocky, the program manager of the Solar Electric Propulsion Technology Application Readiness program, for his support and to the XFS team members without whom the XFS would not have happened. The research described in this paper was carried out by the Jet Propulsion Laboratory, California Institute of Technology, under a contract with NASA.

References

- ¹Sovey, J. S., Hamley, J. A., Haag, T. W., Patterson, M. J., Pencil, E. J., Peterson, T. T., Pinero, L. R., John, L., Rawlin, V. K., and Sarmiento, C. J., "Development of an Ion Thruster and Power Processor for New Millennium's Deep Space 1 Mission," AIAA Paper 97-2778, June 1997.
- ²Polk, J. E., Kakuda, R. Y., Anderson, J. R., Brophy, J. R., Rawlin, V. K., Patterson, M. J., Sovey, J. S., and Hamley, J. A., "Validation of the NSTAR Ion Propulsion System on the Deep Space One Mission: Overview and Initial Results," AIAA Paper 99-2274, June 1999.
- ³Marcucci, M. G., and Polk, J. E., "NSTAR Xenon Ion Thruster on DS1: Ground and Flight Tests," 8th International Conf. on Ion Sources, American Inst. of Physics, Kyoto, Japan, Sept. 1999 (I-18).
- ⁴Christensen, J. A., Benson, G., Bond, T., Gallagher, J., and Matranga, M., "The NSTAR Ion Propulsion Subsystem for DS1," AIAA Paper 99-2972, June 1999.
- ⁵Engelbrecht, C. S., "NSTAR Xenon Feed System (XFS) Technical Requirements Document (TRD)," NSTAR Document ND-330, NASA, Jan. 1997.
- ⁶Bushway, E., III, Engelbrecht, C., and Ganapathi, G., "NSTAR Ion Engine Xenon Feed System: Introduction to System Design and Development," International Electric Propulsion Conf., IEPC 97-044, Aug. 1997.
- ⁷Reid, R. C., Prausnitz, J. M., and Sherwood, T. K., *The Properties of Gases and Liquids*, 3rd ed., McGraw-Hill, New York, 1977, pp. 26-68.
- ⁸Friend, D. G., "NIST Standard Reference Database 12: NIST Thermophysical Properties of Pure Fluids, Ver. 3.0 Users' Guide," National Inst. of Standards and Technology, U.S. Dept. of Commerce, Gaithersburg, MD, Sept. 1992.

J. A. Martin
Associate Editor